Inorganic Chemistry

Article

pubs.acs.org/IC

Copper, Indium, Tin, and Lead Complexes with Fluorinated Selenolate Ligands: Precursors to MSe_x

Kareem Holligan, Patrick Rogler, David Rehe, Michael Pamula, Anna Y. Kornienko, Thomas J. Emge, Karsten Krogh-Jespersen, and John G. Brennan*

Department of Chemistry and Chemical Biology, Rutgers, The State University of New Jersey, New Brunswick, New Jersey 08903, United States

Supporting Information

ABSTRACT: Reductive cleavage of $C_6F_5SeSeC_6F_5$ with elemental M (M = Cu, In, Sn, Pb) in pyridine results in the formation of $(py)_4Cu_2(SeC_6F_5)_2$, $(py)_2In(SeC_6F_5)_3$, $(py)_2Sn(SeC_6F_5)_2$, and $(py)_2Pb(SeC_6F_5)_2$. Each group adopts a unique structure: the Cu(I) compound crystallizes as a dimer with a pair of bridging selenolates, two pyridine ligands coordinating to each Cu(I) ion, and a short Cu(I)−Cu(I) distance (2.595 Å). The indium compound crystallizes as monometallic five-coordinate $(py)_2In(SeC_6F_5)_3$ in a geometry that approximates a trigonal bipyramidal structure with two axial pyridine ligands and three selenolates. The tin and lead derivatives $(py)_2M(SeC_6F_5)_2$ are also monomeric, but they adopt nearly octahedral geometries with trans pyridine ligands, a pair of cis-selenolates, and two "empty" cis-positions on the octahedron that are oriented toward extremely remote selenolates (M−Se = 3.79 Å (Sn), 3.70 Å (Pb)) from adjacent molecules. Two of the four compounds (Cu, In) exhibit intermolecular $\pi-\pi$ stacking arrangements in the solid state, whereas the stacking of molecules for the other two compounds (Sn, Pb) appears to be based upon molecular shape and crystal packing forces. All compounds are volatile and decompose at elevated temperatures to give MSe_x and $Se(C_6F_5)_2$.The electronic structures of the dimeric Cu compound and monomeric $(py)_2M(SeC_6F_5)_2$ (M = Sn, Pb) were examined with density functional theory calculations.

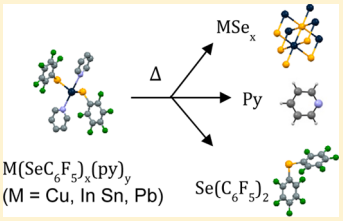

INTRODUCTION

Aromatic $\pi-\pi$ stacking interactions[1] represent an underexplored variable that can potentially be controlled to deliver important materials in new forms, whether it be molecular precursors to compound semiconductors,[2] quantum dots,[3] or two-dimensional materials.[4] Fluorinated arene ligands are likely to engage in $\pi-\pi$ interactions because of the polar nature of the C−F bond. These fluorinated rings impart useful characteristics,[5] including superior solubility/volatility properties and the stabilization of elements in high oxidation states.

Fluorinated phenoxides[6] and thiolates[7] have been used extensively to make stable compounds with metals from every part of the periodic chart, but the analogous fluorinated selenolate chemistry is considerably less developed. The SeC_6F_5 (SeAr) ligand is not commercially available as either the selenol or the diselenide, but a reliable synthesis of $C_6F_5Se-SeC_6F_5$ has been reported.[8] There exists a description of $Tl(SeC_6F_5)$ and heterometallic M/Tl compounds[9] with SeC_6F_5 ligands that contain dative Tl−F interactions, a mer-octahedral lanthanide compound with a significant structural trans influence,[9b] and a recent description of $M(SeC_6F_5)_2$ compounds with the group 12 metals Zn, Cd, and Hg.[10]

In the group 12 work, there was a clear tendency for all three products to crystallize with $\pi-\pi$ stacking arrangements, either as discrete molecules or coordination polymers, as has often been noted in related thiolate chemistry.[11,12] To further explore the chemistry of this ligand, and to examine the possibility of using these $\pi-\pi$ interactions to influence molecular structure, we extended our investigation and describe here the synthesis and characterization of Cu(I), Sn(II), Pb(II), and In(III) compounds with the perfluorinated benzeneselenolate and the subsequent thermolysis behavior of these compounds.

EXPERIMENTAL SECTION

General Methods. All syntheses were performed under ultrapure nitrogen (Welco Praxair), using conventional drybox or Schlenk techniques. Pyridine (Aldrich) was purified with a dual column Solv-Tek solvent purification system and collected immediately prior to use. $Se_2(C_6F_5)_2$ was prepared according to literature procedures.[8] Sn, Pb, Cu, and In metals (Aldrich) were purchased and used as received. Melting points were recorded in sealed capillaries and are uncorrected. IR spectra were recorded on a Thermo Nicolet Avatar 360 FTIR spectrometer from 4000 to 450 cm^{-1} as mineral oil mulls on CsI plates. UV−vis absorption spectra were recorded on a Varian DMS 100S spectrometer with the samples dissolved in pyridine, placed in either a 1.0 mm × 1.0 cm Spectrosil quartz cell or a 1.0 cm^2 special optical glass cuvette, and scanned from 190−800 nm. All NMR data were collected on a Varian VNMRS 500 spectrometer at 25 °C with the compounds dissolved in deuterated dimethyl sulfoxide. ^1H and ^{19}F NMR spectra were obtained at 499 and 476 MHz, respectively; ^{77}Se NMR spectra were acquired with a longer relaxation delay (4.0 s) together with an extended number of scans (2056) in fluorine-decoupled mode at 95 MHz using $(SePh)_2$ as external standard. Electrospray ionization mass spectrometry (MS) data were recorded on a Thermo Finnigan LCQ DUO system with the sample dissolved

Received: March 3, 2015
Published: August 28, 2015

DOI: 10.1021/acs.inorgchem.5b00452
Inorg. Chem. 2015, 54, 8896−8904

Table 1. Summary of Crystallographic Details for 1−4

compound	1	2	3	4
empirical formula	$C_{32}H_{20}Cu_2F_{10}N_4Se_2$	$C_{33}H_{15}F_{15}InN_3Se_3$	$C_{22}H_{10}F_{10}N_2Se_2Sn$	$C_{22}H_{10}F_{10}N_2PbSe_2$
fw	935.52	1090.18	768.93	857.43
space group	$P\bar{1}$	$P2_1/n$	$C2/c$	$C2/c$
a (Å)	7.846(4)	13.037(1)	19.209(3)	19.354(3)
b (Å)	9.932(6)	18.940(2)	5.2539(9)	5.1931(7)
c (Å)	11.707(7)	14.175(1)	24.187(4)	24.613(4)
α (deg)	113.11(1)			
β (deg)	90.91(1)	99.696(2)	108.549(2)	108.569(2)
γ (deg)	98.10(1)			
V (Å^3)	828.2(8)	3450.3(5)	2314.2(7)	2345.0(6)
Z	1	4	4	4
D (calcd) (g/cm^{-3})	1.876	2.099	2.207	2.429
temperature (K)	100(2)	100(2)	100(2)	100(2)
λ (Å)	0.710 73	0.710 73	0.710 73	0.710 73
abs coeff (mm^{-1})	3.569	3.963	4.346	10.394
$R(F)^a$ [$I > 2\sigma(I)$]	0.046	0.026	0.030	0.0238
$R_w(F^2)^b$ [$I > 2\sigma(I)$]	0.120	0.061	0.064	0.057

$^a R(F) = \sum||F_o| - |F_c||/\sum|F_o|$. $^b R_w(F^2) = \{\sum[w(F_o^2 - F_c^2)^2]/\sum[w(F_o^2)^2]\}^{1/2}$. Additional crystallographic details are given in the Supporting Information.

in a 10:1 MeOH/CH_3COOH mixture. Mass spectra were acquired in the negative ion detection mode scanning a mass range from m/z = 150 to m/z = 1000. In the case of isotopic patterns, the value given is for the most intense peak. Powder X-ray diffraction data were obtained on a Bruker HiStar area detector using Cu Kα radiation from a Nonius 571 rotating-anode generator. Elemental analyses were performed by Quantitative Technologies, Inc. (Whitehouse, NJ).

Synthesis of (py)$_4$Cu$_2$(SeC$_6$F$_5$)$_2$ (1). Cu (0.032 g, 0.50 mmol), Hg (0.014 g, 0.070 mmol), and $(SeC_6F_5)_2$ (0.12 g, 0.25 mmol) were added to pyridine (20 mL), and the mixture was stirred at room temperature for 3 d. The solution was filtered to remove Hg, then concentrated to ∼8 mL, layered with ∼20 mL of hexanes, and cooled to ca. 2 °C, to give yellow crystals (0.17 g, 73%) that melted at 102 °C and decomposed at 160 °C. IR: 2944 (s), 2881 (w), 1509 (w), 700 (m), 458 (m), 430 (s), 415 (s), 413 (w), 405 (m) cm^{-1}. UV−vis: This compound shows an optical absorption maximum at 570 nm. Anal. Calcd for $C_{32}H_{20}F_{10}N_4Cu_2Se_2$: C, 41.0; H, 2.10; N, 5.98. Found: C, 41.3; H, 2.31; N, 5.54%. ^{1}H NMR (ppm): 8.67 (s, 2H), 7.82 (t, J = 9.2, 6.4 Hz, 1H), 7.43 (s, 2H). ^{19}F NMR (ppm): −125.26 (d, J = 22.1 Hz, 2F), −162.29 (t, J = 21.2 Hz, 1F), −164.70 (t, J = 22.1 Hz, 2F). No ^{77}Se NMR signal was observed.

Synthesis of (py)$_2$In(SeC$_6$F$_5$)$_3$·py (2). In (0.057 g, 0.50 mmol), Hg (0.013 g, 0.065 mmol), and $(SeC_6F_5)_2$ (0.37 g, 0.75 mmol) were combined in pyridine (20 mL), and the mixture was stirred at room temperature for 15 d. The solution was filtered to remove Hg, concentrated to ∼8 mL, layered with ∼20 mL of hexanes and cooled (2 °C) to give colorless crystals (0.37 g, 56%; mp 106 °C; dec 198 °C). IR: 2975 (s), 2880 (w), 2843 (w), 1602 (m), 1508 (m), 1483 (s), 1217 (s), 1007 (w), 1070 (m), 973 (m), 816 (m), 702 (m), 627 (w), 413 (w) cm^{-1}. UV−vis: This compound shows an optical absorption maximum at 330 nm. Anal. Calcd for $C_{33}H_{15}F_{15}InN_3Se_3$: C, 36.3; H, 1.39; N, 3.85. Found: C, 36.2; H, 1.39; N, 4.09%. ^{1}H NMR (ppm): 8.56 (dt, J = 4.0, 1.7 Hz, 2H), 7.76 (dd, J = 5.6, 4.0, 1.4 Hz, 1H), 7.36 (tt, J = 15.2, 7.6, 1.7 Hz, 2H). ^{19}F NMR (ppm): −124.23 (d, J = 28.2 Hz, 2F), −159.22 (t, J = 28.2 Hz, 1F), −163.84 (broad s, 2F). ^{77}Se {^{19}F} NMR (ppm): 382.5.

Synthesis of (py)$_2$Sn(SeC$_6$F$_5$)$_2$ (3). Sn (0.24 g, 2.01 mmol), Hg (0.020 g, 0.10 mmol), and $(SeC_6F_5)_2$ (0.99 g, 2.01 mmol) were combined in pyridine (ca. 25 mL), and the mixture was stirred at room temperature for 16 d. The solution was heated to 60 °C, filtered, concentrated to ∼5 mL, and cooled to room temperature to give light orange crystals (0.91 g, 84%) that began to melt at 110 °C, melted completely at 119 °C, and decomposed at 229 °C. IR: 2957 (s), 2284 (m), 1607 (w), 1593 (w), 1510 (s), 1462 (s), 1377 (s), 1213 (m), 1153 (m), 1083 (m), 1031 (m), 1010 (m), 971 (s), 815 (m), 751 (m), 723 (m), 700 (s), 617 (s) cm^{-1}. UV−vis: This compound shows a broad optical absorption maximum at 450 nm. Anal. Calcd for $C_{22}H_{10}N_2F_{10}SnSe_2$: C, 34.4; H, 1.31; N, 3.64; Found: C, 33.6; H, 1.37; N, 3.69%. ^{1}H NMR (ppm): 8.56 (m, 2H), 7.78 (tt, J = 7.6, 1.8 Hz, 1H), 7.37 (m, 2H). ^{19}F NMR (ppm): −126.11 (d, J = 28.2 Hz, 2F), −160.63 (broad s, 1F), −163.84 (t, J = 28.2 Hz, 2F). ^{77}Se {^{19}F} NMR (ppm): 75.98.

Synthesis of (py)$_2$Pb(SeC$_6$F$_5$)$_2$ (4). Pb (0.21 g, 1.0 mmol) and $(SeC_6F_5)_2$ (0.49 g, 1.0 mmol) were combined in pyridine (15 mL) with a catalytic amount of Hg (ca. 0.05 g). The resulting mixture was stirred until all the metal powder was completely consumed (7 d). The deep orange solution was separated from a dark gray precipitate by hot filtration at 70 °C and cooled to room temperature to give brown crystals (0.74 g, 70%) that turned red at 160 °C and decomposed at 205 °C. IR: 2922(s), 2854(s), 1592(m), 1509(s), 1478(s), 1442(s), 1377(m), 1359(m), 1329(w), 1214(w), 1152(w), 1081(m), 1065(m), 1030(w), 1000(m), 969(s), 814(s), 750(m), 701(s), 617(m) cm^{-1}. This compound gives a broad optical absorption maximum at 451 nm. Anal. Calcd for $C_{22}H_{10}N_2F_{10}PbSe_2$: C, 30.7; H, 0.85; N, 3.08; Found: C, 30.5; H, 0.87; N, 3.11%. ^{1}H NMR (ppm): 8.55 (m, 2H), 7.76 (m, 1H), 7.36.0 (tt, J = 15.6, 7.6, 1.8 Hz 2H). ^{19}F NMR (): −126.07 (d, J = 28.2 Hz, 2F), −161.18 (broad s, 1F), −164.25 (t, J = 28.2 Hz, 2F). ^{77}Se {^{19}F} NMR (ppm): 75.76.

Thermolysis. Typically, a sample of **1**−**4** (ca. 20 mg) was placed in a quartz thermolysis tube that was sealed under vacuum, and the sample end was placed into a model 847 Lindberg tube furnace. The "cold" end of the glass tube was held at −196 °C by immersion in liquid nitrogen. The sample was heated to 650 °C at a ramp rate of 10 °C/min and then held at 650 °C for 5 h, at which time it was cooled to 25 °C at a rate of 3.5 °C/min. For **1**, the black powder that was formed at the sample end of the quartz tube was identified as Cu_9Se_5 with multiple phases present; the structure most identified with a berzelianite derivative.[13] The resultant solid for **2** was identified as In_2Se_3;[14] **3** gave SnSe,[15] and **4** gave PbSe.[16] Gas chromatography (GC)MS analysis of the volatile products identified py and $Se(C_6F_5)_2$ (m/z = 413) in all four cases.

X-ray Structure Determination. Single-crystal X-ray data for **1**−**4** were collected on a Bruker Smart APEX CCD diffractometer with graphite monochromatized Mo Kα radiation (λ = 0.710 73 Å) at 100 K. Crystals were immersed in mineral oil and examined at low temperatures. The data were corrected for Lorenz effects, polarization, and absorption, the latter by a multiscan (SADABS)[17] method. The structures were solved by direct methods (SHELXS86).[18] All non-

DOI: 10.1021/acs.inorgchem.5b00452
Inorg. Chem. 2015, 54, 8896−8904

hydrogen atoms were refined (SHELXL97)[19] based upon F_{obs}.[2] All hydrogen atom coordinates were calculated with idealized geometries (SHELXL97). Scattering factors (f_o, f', f'') are as described in SHELXL97. Crystallographic data and final R indices for **1**–**4** are given in Table 1. Molecular visualization by use of Mercury CSD diagrams[20] for **1**, **2**, and the common structure for **3** and **4** are shown in Figures 1a, 2a, and 3a, respectively. Packing diagrams for **1**, **2**, and the common structure of **3** and **4** are given in Figures 1b, 2b, and 3b, respectively.[21] Additional crystallographic details are provided in Supporting Information.

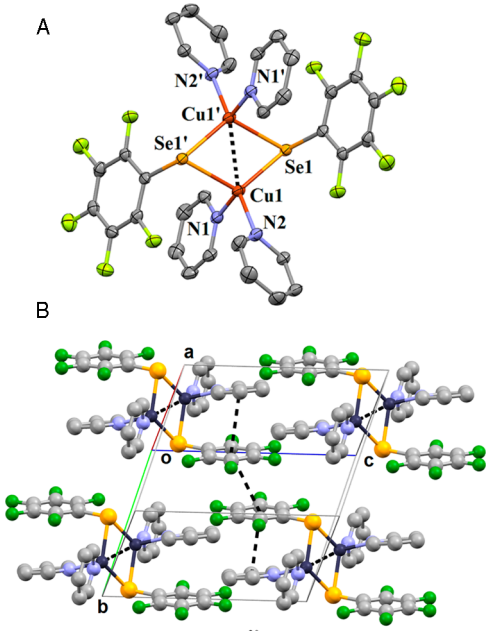

Figure 1. (a) Molecular visualization of dimeric $(py)_4Cu_2(SeC_6F_5)_2$ in **1**, with the H atoms removed for clarity and ellipsoids at the 50% probability level. Significant bond lengths [Å] and angles [deg]: Cu(1)–N(2), 2.048(3); Cu(1)–N(1), 2.096(3); Cu(1)–Se(1), 2.4648(12); Cu(1)–Se(1)′, 2.5248(13); Cu(1)–Cu(1)′, 2.5952(14) (see dashed line); Se(1)–C(1), 1.929(4); Se(1)–Cu(1)′, 2.5248(13); N(2)–Cu(1)–N(1), 104.34(13); N(2)–Cu(1)–Se(1), 119.88(10); N(1)–Cu(1)–Se(1), 98.40(10); N(2)–Cu(1)–Se(1)′, 109.40(10); N(1)–Cu(1)–Se(1)′, 104.64(8); Se(1)–Cu(1)–Se(1)′, 117.33(2); N(2)–Cu(1)–Cu(1)′, 142.77(10); N(1)–Cu(1)–Cu(1)′, 112.62(9); Se(1)–Cu(1)–Cu(1)′, 59.80(4); Se(1)′–Cu(1)–Cu(1)′, 57.53(3). Symmetry transformation used to generate equivalent (′) atoms: $-x+1$, $-y$, $-z$.(b) Ball-and-stick drawing[20] of the crystal packing in **1** as viewed approximately along the crystallographic **a**+**b** diagonal with the **c** axis along the page. Likely $\pi\cdots\pi$ interactions as indicated by dashed lines between ring centroids (see text), form isolated triplets of contacts: two py···SeAr distances of 3.51 Å and one SeAr···SeAr distance of 3.61 Å. The H atoms are omitted for clarity. Atom types are as indicated by colors in (a).

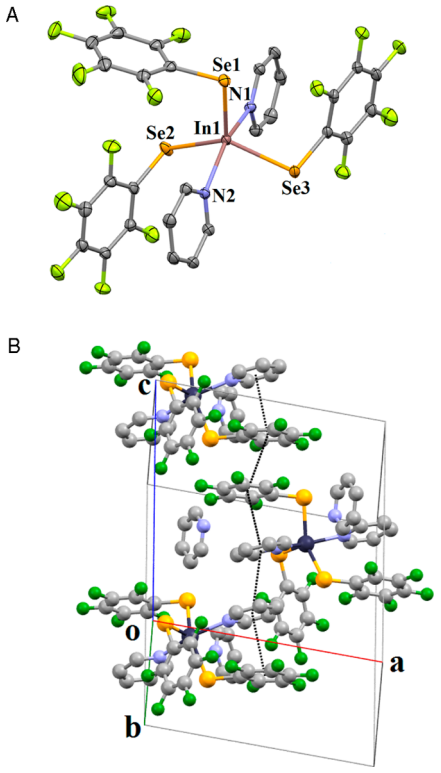

Figure 2. (a) Molecular visualization of the $(py)_2In(SeC_6F_5)_3$ molecule of **2**, with the H atoms removed for clarity and ellipsoids at the 50% probability level. Selected bond lengths [Å] and angles [deg]: In(1)–N(2), 2.3594(14); In(1)–N(1), 2.3714(15); In(1)–Se(1), 2.5630(3); In(1)–Se(2), 2.5919(3); In(1)–Se(3), 2.5980(3); N(2)–In(1)–N(1), 156.54(5); N(2)–In(1)–Se(1), 105.15(4); N(1)–In(1)–Se(1), 98.28(4); N(2)–In(1)–Se(2), 90.21(4); N(1)–In(1)–Se(2), 80.27(4); Se(1)–In(1)–Se(2), 116.540(8); N(2)–In(1)–Se(3), 82.13(3); N(1)–In(1)–Se(3), 90.96(4); Se(1)–In(1)–Se(3), 104.506(8); Se(2)–In(1)–Se(3), 138.803(9). (b) Ball-and-stick drawing[20] of the crystal packing in **2** as viewed approximately along the crystallographic **b**+**c** diagonal with the **a** axis along the page. The likely $\pi\cdots\pi$ interactions in **2** form a 1D array of contacts along the **c** axis. The repeating quartet of distances are 3.55, 3.79, 3.70, and 3.64 Å between respective ring centroids (shown by dashed lines propagating from lower to upper in the figure) for the SeAr···py, py···py, py···SeAr, and SeAr···SeAr interactions, respectively (see text). The py molecules of solvation are shown, but all H atoms are omitted for clarity. Atom types are as indicated by colors in (a).

Computational Details. Electronic structure calculations, facilitated by the GaussView[22] and Gaussian 09[23] suites of programs, were performed on **1**, **3**, and **4**. We employed density functional theory (DFT)[24] with the M06,[25] M06-L,[25a] PBE,[26] and B3LYP[27] exchange-correlation functionals. For Pb, Sn, Cu, and Se, we applied the Wadt–Hay relativistic effective (small) core potentials[28] and the LANL2TZ basis sets[28,29] augmented by one f-type function and a complete set of diffuse spdf functions;[30] 6-311+G(d,p) basis sets were used for F, N, C, and H atoms.[31] Standard procedures were employed to obtain the optimized geometries, and normal-mode analysis was performed to verify the nature of the located stationary points as true minima. Increased atomic grid sizes (pruned (99 590) grids) were used for the numerical integrations to enhance computational stability and accuracy of geometry optimizations and vibrational frequency calculations (grid = ultrafine option). Natural bond orbital (NBO) analysis was performed with NBO5, version 5.9.[32,33]

RESULTS AND DISCUSSION

Reaction of M (M = Cu, In, Sn, Pb) with $C_6F_5Se–SeC_6F_5$ in pyridine leads to the reductive cleavage of the Se–Se bond and the formation of metal selenolate compounds that crystallize as pyridine adducts. This is a particularly attractive synthetic approach due to the minimal number of reagents involved, the relatively high yields obtained, and the ease with which the product can be isolated since there are no solid-state byproducts.

With Cu, reduction over a period of days followed by saturation of the solution after the Cu had been consumed Reaction 1, leads to the isolation of $(py)_4Cu_2(SeC_6F_5)_2$ (**1**) in high yield. This compound was characterized by conventional spectroscopic methods and low-temperature single-crystal X-

DOI: 10.1021/acs.inorgchem.5b00452
Inorg. Chem. 2015, 54, 8896–8904

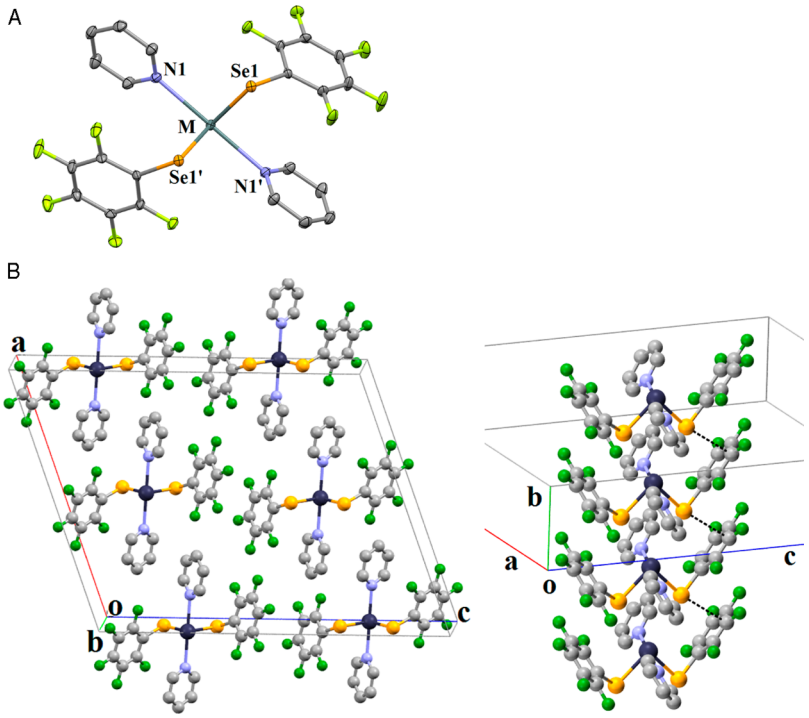

Figure 3. (a) Molecular visualization of the common structure $(py)_2M(SeC_6F_5)_2$, for **3** (M = Sn) or for **4** (M = Pb), with the H atoms removed for clarity and ellipsoids at the 50% probability level. Significant bond lengths [Å] and angles [deg] for **3**: Sn(1)−N(1), 2.553(2); Sn(1)−N(1)′, 2.553(2); Sn(1)−Se(1)′, 2.6637(5); Sn(1)−Se(1), 2.6637(5); Se(1)−C(1), 1.911(3); Se(1)−Sn(1)′, 2.6637(5); N(1)−Sn(1)−N(1)′, 176.90(10); N(1)−Sn(1)−Se(1)′, 86.38(5); N(1)′−Sn(1)−Se(1)′, 91.37(5); N(1)−Sn(1)−Se(1), 91.37(5); N(1)′−Sn(1)−Se(1), 86.38(5); Se(1)′−Sn(1)−Se(1), 86.804(19). Significant bond lengths [Å] and angles [deg] for **4**: Pb(1)−N(1), 2.655(2); Pb(1)−N(1)′, 2.655(2); Pb(1)−Se(1), 2.7551(4); Pb(1)−Se(1)′, 2.7551(4); N(1)−Pb(1)−N(1)′, 179.44(11); N(1)−Pb(1)−Se(1), 92.12(5); N(1)′−Pb(1)−Se(1), 87.46(5); N(1)−Pb(1)−Se(1)′, 87.47(5); N(1)′−Pb(1)−Se(1)′, 92.12(5); Se(1)−Pb(1)−Se(1)′, 86.184(16). Symmetry transformation used to generate equivalent atoms: $-x + 1$, y, $-z + 1/2$. (b) Ball-and-stick drawing[20] of the crystal packing for **3** and **4** (M = Sn and Pb) as viewed approximately along the crystallographic **b** axis (left) and **a**+**c** diagonal axis (right). There are no short contact distances that indicate significant $\pi\cdots\pi$ interactions, and the closest interligand contact is 3.53 Å between a Se atom and a C atom of two SeAr groups related by **b**-axis translation, as indicated by the dashed lines (right). The H atoms are omitted for clarity. Atom types are as indicated by colors in (a).

ray diffraction. The molecular structure of **1** is shown in Figure 1a with significant geometrical parameters given in the figure caption.

$$Cu + C_6F_5SeSeC_6F_5 \xrightarrow{py} [(py)_2Cu(SeC_6F_5)]_2 \quad (1)$$

The Cu compound is a dimer, with a central Cu−Cu separation of 2.595(1) Å; there are two bridging selenolates and two pyridine donors saturating the primary coordination sphere. When compared to over 360 structures in the Cambridge Structural database (CSD) with bridged pairs of Cu(I) atoms, this Cu−Cu separation is consistent with the range of values reported, 2.4 Å to 3.0 Å, which contain several instances of the longer bridging iodide atoms, and somewhat shorter than the mean value, 2.72 Å. This separation is also somewhat shorter than the mean value of 2.71 Å for the 10 instances of neutral dimer compounds in the CSD with four-coordinate Cu(I) and bridging O-, S-, or Se-containing μ^2 ligands.[34] There exist Cu(II) compounds with fluorinated thiolate ligands: tetrahedral pyrazolylborate compounds with monodentate thiolates[35] and an octahedral cis bis-thiolate compound with a tetradentate amine ligand.[36] One of the Cu(II) pyrazolylborate compounds was also reduced to give a Cu(I) product, again with a tetrahedral geometry and a terminal thiolate.

Compound **1** has a yellow color because of an electronic transition with an absorption maximum at 570 nm; this absorption has been attributed to a ligand-to-metal charge transfer transition in previous descriptions of Cu(I) compounds with selenolate ligands.[34e] The NMR spectra suggest that there are dynamic processes that influence line shapes (noted also for the Sn and Pb compounds), but conditions for obtaining classical slow or fast exchange spectra could not be determined because of problems with either solubility or thermal stability.

The dimeric motif found in **1** is often observed in Cu(I) chalcogenolate compounds; although depending on the steric demands of the ancillary ligands (or the lack thereof), compounds have been noted with Cu_4, Cu_6, and polymeric frameworks.[34e−j] Most of these compounds contain metallophilic interactions, even in the presence of bulky phosphine ligands and sterically demanding chalcogenolates that typically favor structures of low nuclearity. Within the lattice of **1**, there are a number of close associations between planar aromatic rings that are consistent with $\pi\cdots\pi$ interactions (e.g., closely stacking, nearly parallel rings with separations less than 3.8 Å and lateral shifts less than 2.3 Å, approximately) or $\sigma\cdots\pi$ interactions (e.g., CH···ring) of aromatic compounds, cf. Figure 1b (the separations given are for segments of the rings that overlap when viewed in projection, and the lateral shifts are for the projected ring centroids). Both the $\pi\cdots\pi$ and the CH···π noncovalent interactions are commonly observed in the crystal structures of aromatic compounds and have been assumed to be a driving force for crystal packing, protein folding, and molecular recognition.[37,38] The likely $\pi\cdots\pi$ interactions of

DOI: 10.1021/acs.inorgchem.5b00452
Inorg. Chem. 2015, 54, 8896−8904

aromatic rings (py or SeAr) along the crystallographic (a−b) diagonal, namely, py1···SeAr···SeAr′···py(1′), are capped in either direction by the $\sigma\cdots\pi$ interactions between the two unique py ligands. For the four $\pi\cdots\pi$ interactions, the central two fluorinated rings are positioned to allow significant overlap with separation of 3.3 and 3.2 Å, dihedral angles of 0° and 120°, and lateral separations of 1.3 and 1.2 Å for SeAr···SeAr′ and SeAr′···py(1′), respectively. A $CH_3\cdots\pi$ interaction, involving the atoms H(12) and C(7) at a distance of 3.1 Å, is observed for py(2′)···py(1) or py(1′)···py(2″). The above sequence repeats upon inversion at (1/2, 1/2, 0) and near py(2) with the H(16)···H(16′) distance at 2.5 Å, slightly longer than the sum of the van der Waals radii (2.4 Å).

Indium metal behaves similarly, reducing $(SeC_6F_5)_2$ over a span of days at room temperature to afford a light yellow solution Reaction 2, from which crystals of the monopyridine solvate of $(py)_2In(SeC_6F_5)_3$ can be isolated by saturating the solution with hexane. This contrasts with earlier fluorinated thiolate literature, where $In(SC_6F_5)_3$ is reported to crystallize from hexane and not react further with pyridine.[39] The structure of **2**, as established by low-temperature X-ray diffraction, is a monomeric distorted trigonal bipyramid with a pair of axial pyridine donors (N(2)−In(1)−N(1) = 156.54(5)°) and three equatorial selenolates distorted from ideal positions [Se(1)−In(1)−Se(2) = 116.540(8); Se(1)−In(1)−Se(3) = 104.506(8); Se(2)−In(1)−Se(3) = 138.803(9)] (Figure 2). While distorted, the three Se−In−Se bond angles still sum to nearly 360° (359.8°). There are continuous one-dimensional (1D) arrays of ring stacking motifs along the *c*-axis in the crystal structure of **2** (Figure 2b), with favorable $\pi-\pi$ interaction geometries for alternating inter- and intramolecular stacking of rings, namely, SeAr(3)···py(1) [3.1 Å separation, 17° dihedral, and 1.1 Å lateral shift], py(1)···py(2′) [3.3 Å separation, 8° dihedral, and 1.9 Å lateral shift], py(2)···SeAr(2) [3.8 Å separation, 15° dihedral, and 0.8 Å lateral shift], and SeAr(2) and SeAr(3′) [3.4 Å separation, 3° dihedral, and 1.2 Å lateral shift].

$$In + 3/2\ C_6F_5SeSeC_6F_5 \xrightarrow{py} (py)_2In(SeC_6F_5)_3 \qquad (2)$$

Indium selenolate geometries are highly sensitive to the coordination environment, with previous reports describing compounds with coordination numbers that range from three to six. There is no structure of a homoleptic In(III) fluorothiolate, but a tetrahedral geometry was observed in $[In(SC_6F_5)_2(OPh)]_2$.[40] Introduction of an R group with extraordinary steric demands (i.e., SeC_6H_2-2,4,6,Bu^t)[41] leads to the formation of three coordinate molecules, while reduction in the size of R leads to distorted tetrahedral dimers with bridging and terminal SeR ligands.[42] The $In(SePh)_4$ anion[43] is more of an ideal tetrahedron, and octahedral (N_3Se_3) geometries are observed with chelating ligands, that is, In(Se-2-$NC_5H_4)_3$.[44] With the fluorinated selenolate ligand, compound **2** is the first $In(SeR)_3$ product to adopt a trigonal bipyramidal geometry.

Tin and lead metals also reduce 1 equiv of the diselenide to give divalent products that were identified as $(py)_2M(SeC_6F_5)_2$ (M = Sn(**3**); Pb(**4**)), Reaction 3, by single-crystal X-ray diffraction.

$$M + C_6F_5SeSeC_6F_5 \xrightarrow{py} (py)_2M(SeC_6F_5)_2 \quad (M = Sn, Pb) \qquad (3)$$

The structures of **3** and **4** (Figure 3a) contain stacks of M(II) atoms that are formally bound to two pyridine and two selenolate ligands and datively bound to the two selenolate ligands bonded to the M(II) atom related to the first by simple translation along the *b*-axis, thus forming an infinite array of octahedrally arranged ligands with two M−Se bonds of ∼2.7 Å, typical lengths of such bonds in M(II) compounds,[34g,45] and two dative M-Se interactions spanning ∼3.7 Å; the same structure was communicated in the structure report of $Pb(SeC_6F_5)_2$.[46] For comparison, the solid-state structure of SnSe is a distorted NaCl lattice with three short (2.77, 2.82, and 2.82 Å) and three long (3.35, 3.35, and 3.47 Å) Sn−Se separations.[45a] The nearly octahedral geometries of these M(II) complexes are reflected in the cis-L−M−L angles of 88.2° (Sn) and 88.6° (Pb). These structures also reveal similar aromatic ring-stacking arrangements as found in **1** with four nearly parallel ligands, namely, two instances of intramolecular SeAr···py on either side of the SeAr···SeAr from crystallographically related (inversion at (1/2, 1/2, 1/2)) $py_2M(II)(SeAr)_2$ units, capped on either end of the stack with CH···SeAr contacts of ∼3.0 Å. For the crystal structures of these M(II) compounds, the separations, dihedrals, and lateral shifts for the unique SeAr···py and SeAr···SeAr′ units are 3.3 Å, 0°, 2.3 Å; 3.2 Å, 8°, 2.5 Å for **3** and 3.4 Å, 0°, 2.4 Å; 3.2 Å, 4°, 2.6 Å for **4**.

While there is literature precedent for selenolates stabilizing Sn(IV) in the preparation of $Sn(SePh)_4$,[45a] reactions with 2 equiv of fluorinated diselenide and Sn metal resulted only in the isolation of the divalent product. This should not imply that the divalent state is particularly stable—in fact, given the fluorinated selenolates of Zn(II), Cd(II), Hg(II),[10] Cu(I), Sn(II), Pb(II), and In(III), only the Sn(II) compound **3** reacts visibly with air, presumably by reducing oxygen to form Sn(IV) oxide products.[47]

There are only a handful of structurally characterized group 14 $M(SeR)_2$ (M = Sn, Pb) compounds in the literature, and within this small number there is an extraordinarily diverse range of coordination environments. The most recent contribution to this molecular class is a remarkable group of two-coordinate $M(SeAr^{ipr}_4)_2$ compounds[48] with acute Se−M−Se bond angles in which the ideal E−M−E bond angles are compressed because of intramolecular dispersion forces. Approaches to ideal right angle bonding similar to **3** and **4** are also found in the pseudo-octahedral arrangements of $[Sn(Se\text{-}2\text{-}NC_5H_4)_2]_n$,[49] in which $[Sn(Se\text{-}2\text{-}NC_5H_4)_2]_2$ units are connected to neighboring dimers with a relatively long (3.618(2) Å) Sn−Se interaction. In this case, deviations from ideal geometries arise from constraints associated with the chelating SePy ligand. Compounds **3** and **4** possess geometries that are most consistent with pure p-orbital metal involvement in M−Se bonding. Structures of divalent compounds have also displayed geometries consistent with the presence of a stereochemically active lone pair on the metal, as seen in the structures of polymeric[45c] $Sn(SePh)_2$, dimeric $M(ESi(SiMe_3)_3)_2$,[45d] and molecular $Pb(SeCH_2CH_2NMe_2)_2$.[45e]

Computations. Using the X-ray structures of **1**, **3**, and **4** as guidance, initial geometries representing monomeric (**3**, **4**) or dimeric (**1**) units were constructed; these trial structures were then optimized employing several functionals (M06, M06-L, PBE, and B3LYP).[22−24] In all cases, the geometry optimizations converged to minima featuring C_i symmetry (**1**) or C_2 symmetry (**3**, **4**; twofold rotation axis bisecting the Se−M−Se angle).

The structural parameter of primary interest in **1** is the short Cu(I)−Cu(I) separation. The optimized geometry produced by the B3LYP functional shows a Cu−Cu distance of 2.614 Å,

DOI: 10.1021/acs.inorgchem.5b00452
Inorg. Chem. 2015, 54, 8896−8904

essentially equal to the experimental value of 2.595 Å; the other functionals applied here lead to even shorter Cu−Cu separations: 2.554 Å (PBE), 2.475 Å (M06-L), and 2.473 Å (M06). Computed Cu−Cu Wiberg bond indices[50] fall in the range from 0.05 (B3LYP) to 0.08 (M06-L); for comparison, the Wiberg indices for the Cu−Se single bonds are computed to be in the range of 0.20−0.23. Both computed (idealized gas phase) and experimental (X-ray) values derived for the Cu(I)−Cu(I) distance are distinctly shorter than the sum of the van der Waals radii (2.80 Å) and close to the sum of the metal atom radii (2.556 Å), suggesting that attractive interactions exist between the Cu atoms.[51] The modest but distinctly nonzero value of the Cu−Cu bond order also supports weak bonding existing between the formally closed-shell, d^{10} Cu(I) ions in **1**.

Optimized values of essential geometrical parameters characterizing the metal coordination geometry in **3** and **4** are summarized in Table 2. The data presented in Table 2

Table 2. Comparison of Experimental and Computed Structures for Monomeric 3 and 4[a]

$(py)_2Sn(SeC_6F_5)_2$					
parameter	X-ray	M06	M06-L	PBE	B3LYP
Sn(1)−N(1)	2.553	2.571	2.577	2.592	2.623
Sn(1)−Se(1)	2.664	2.694	2.694	2.700	2.700
Se(1)−C(1)	1.911	1.918	1.914	1.926	1.927
N(1)−Sn(1)−N(1)′	176.9	171.7	168.2	173.4	174.2
N(1)−Sn(1)−Se(1)′	86.4	84.0	82.0	85.3	87.6
N(1)−Sn(1)−Se(1)	91.4	89.9	89.3	89.7	88.1
Se(1)−Sn(1)−Se(1)′	86.8	85.4	84.3	84.0	86.2
$(py)_2Pb(SeC_6F_5)_2$					
parameter	X-ray	M06	M06-L	PBE	B3LYP
Pb(1)−N(1)	2.655	2.646	2.654	2.676	2.716
Pb(1)−Se(1)	2.755	2.744	2.744	2.759	2.765
Se(1)−C(1)	1.914	1.916	1.913	1.924	1.924
N(1)−Pb(1)−N(1)′	179.4	172.9	168.9	174.9	177.4
N(1)−Pb(1)−Se(1)′	87.5	84.1	81.4	87.9	88.5
N(1)−Pb(1)−Se(1)	92.1	90.7	90.4	88.3	89.6
Se(1)−Pb(1)−Se(1)′	86.2	85.8	85.6	85.0	86.6

[a]Bond lengths in angstroms, angles in degrees.

demonstrate that all four functionals applied here produce optimized monomer structures for **3** and **4** that are very similar to the experimentally determined structures with respect to the local geometries observed around the central metal atoms. The more elaborate, widely applicable M06 and M06-L functionals[22] lead to more compact geometries (also noticeable in the optimized Cu−Cu distances in **1**, vide supra) in which the rings in adjacent SeAr-py pairs are approximately parallel with an edge-to-edge distance of 3.5−3.6 Å, indicating the presence of some $\pi(C_6F_5)$-π(py) overlap; the optimized geometries arising from use of the older, less comprehensive PBE and B3LYP functionals are more open and extended. The M06 and M06-L functionals clearly provide an improved account of the medium-range correlation energy (and hence dispersion).[22b,c] In particular, the B3LYP optimized structures of both **3** and **4** show the aromatic rings rotated to such an extent that intramolecular π−π interactions appear to be minimal (see Figure S-1 in Supporting Information), reflecting the absence of any consideration of dispersion interactions in this functional. Thus, the basic coordination geometry for **3** and **4** does not appear to be imposed by the crystal lattice; intramolecular π−π interactions appear to be sufficiently strong to engender some overlap of SeAr-py rings in isolated (idealized gas phase) $(py)_2M(SeC_6F_5)_2$ monomeric units. However, the full extent of π−π interactions and hence the final values of the dihedral angles and overlap attained by the aromatic rings in the crystals of **3** and **4** are undoubtedly determined by the lattice so as to maximize overall thermodynamic stability (cf. Figure 3).

We analyzed the M06 wave functions in some detail using the NBO partitioning and analysis schemes.[32] Applying default program settings, the wave function for **3** localizes well with more than 98% of the total number of electrons placed in Lewis-type localized orbitals and less than 2% appearing in valence and Rydberg non-Lewis orbitals. Ignoring occupancies less than 0.02 e, the natural electronic configurations for the metal and immediate ligated atoms are Sn: (core)$5s^{1.84}5p^{1.28}$; Se: (core)$4s^{1.78}4p^{4.32}4d^{0.02}$; and N: (core)$2s^{1.35}2p^{4.17}$, giving rise to natural net charges of Sn: +0.85; Se: −0.14; and N: −0.54, respectively. The two equivalent Sn−Se bond orbitals each contain 1.92 e and may be characterized as having formed from Sn and Se hybrid orbitals with contributing weights of 22% and 78%, respectively. The hybridization of the Sn orbital used for Se bonding is effectively $sp^{18.6}$ (corresponding to ca. 5% s- and 94% p-character); the Se partner orbital also has substantial p-orbital content with an effective hybridization of $sp^{6.8}$ (corresponding to ca. 13% s- and 86% p-character). Participation by d- and f-functions in these hybrids is slightly higher for Se than for Sn but is overall insignificant. Rounding out the occupied Lewis orbitals involving Sn is a lone pair orbital with an occupancy of 1.98 e and $sp^{0.1}$ hybridization (corresponding to ca. 90% s- and 10% p-character). The Kohn−Sham molecular orbital for **3**, which most closely approximates this highly localized Sn lone pair, is illustrated in Figure 4.

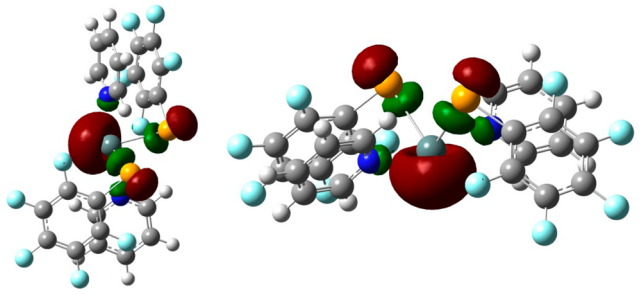

Figure 4. Side and top views of the Kohn−Sham molecular orbital for **3**, which most closely approximates a localized 5s lone pair on the central Sn atom.

The overwhelming extent of 5p orbital character present in the Sn hybrids used for Sn−Se bonding, combined with the existence of the 5s-like lone pair on Sn, explains the nearly 90° value of the Se−Sn−Se angle (computed and observed). In this localized orbital picture, the interaction between Sn and N(py) becomes mostly electrostatic in nature. In a coordinate system where the *z*-axis (the C_2 rotation axis) bisects the Se−Sn−Se angle and the triad N−Sn−N approximately defines the *y*-axis, the atomic orbital occupancies for Sn are

DOI: 10.1021/acs.inorgchem.5b00452
Inorg. Chem. 2015, 54, 8896−8904

$5s^{1.84}5p_x^{0.37}5p_y^{0.25}5p_z^{0.67}$, that is, very low occupancy in the p_y orbital, which potentially interacts with the N(py) lone pairs. The Wiberg bond index[50] for the Sn−N bond is only 0.17, indicating limited covalent character in the Sn−N bond; for comparison, the Wiberg Sn−Se bond index is 0.69. The total Wiberg bond index for Sn (1.91) is comparable to that of Se (1.93) but, of course, much smaller than, for example, that of N (3.15).

The NBO analysis of **4** proceeds in a manner entirely analogous to that just described for **3**. The parameter values obtained for **4** typically differ by only 1−2% from their counterparts in **3** (see Supporting Information for details).

Thermolysis. The potential utility of these molecules as precursors to new forms of compound semiconductors inspires an investigation into their thermolysis behavior. For Sn, Pb, and In, thermal decomposition proceeded as expected with the formation of MSe/In_2Se_3 phases and the elimination of $Se(C_6F_5)_2$ as detected by GC/MS. This reactivity parallels previous descriptions of covalent metal chalcogenolate thermolyses, with the exception of $Zn(SC_6F_5)_2$, which afforded ZnF_2. In contrast, the Cu reaction gave a mixture of $CuSe_x$ phases. Nonstoichiometric CuSe products have been noted previously in molecular thermolyses, with product distributions that depend upon thermolysis conditions.[34j]

CONCLUSIONS

The fluorinated selenolate ligand SeC_6F_5 forms easily crystallized pyridine coordination compounds with the group 11, 13, and 14 metals Cu, In, Sn, and Pb. These compounds expand the already diverse range of metal selenolate structural types found in each group, with extensive $\pi-\pi$ stacking evident throughout all structures. All compounds decompose to give solid-state MSe at elevated temperatures, with the elimination of $Se(C_6F_5)_2$.

ASSOCIATED CONTENT

Supporting Information

The Supporting Information is available free of charge on the ACS Publications website at DOI: 10.1021/acs.inorgchem.5b00452.

X-ray crystallographic information including cell data, atomic coordinates, bond lengths, bond angles, and torsion angles for the crystal structures of **1**, **2**, **3**, and **4**. (PDF)

Illustrated structure and optimized geometries of **3**, NBO analysis of **4**. (PDF)

AUTHOR INFORMATION

Corresponding Author

*E-mail: bren@rci.rutgers.edu.

Author Contributions

The manuscript was written through contributions of all authors.

Notes

The authors declare no competing financial interest.

ACKNOWLEDGMENTS

We acknowledge the support of NSF (CHE-0747165). K.H., M.P., and D.R. received support from the Rutgers Aresty Chemistry Scholars Program.

REFERENCES

(1) (a) Pace, C. J.; Gao, J. M. *Acc. Chem. Res.* **2013**, *46* (4), 907−915. (b) Kishikawa, K. *Isr. J. Chem.* **2012**, *52* (10), 800−808.

(2) (a) Brennan, J. G.; Siegrist, T.; Carroll, P. J.; Stuczynski, S. M.; Reynders, P.; Brus, L. E.; Steigerwald, M. L. *Chem. Mater.* **1990**, *2* (4), 403−409. (b) Boadi, N. O.; Malik, M. A.; O'Brien, P.; Awudza, J. A. M. *Dalt. Trans.* **2012**, *41* (35), 10497−10506. (c) Ritch, J. S.; Chivers, T.; Afzaal, M.; O'Brien, P. *Chem. Soc. Rev.* **2007**, *36* (10), 1622−1631. (d) Sharma, R. K.; Kedarnath, G.; Wadawale, A.; Betty, C. A.; Vishwanadh, B.; Jain, V. K. *Dalton Trans.* **2012**, *41* (39), 12129−12138. (e) Ramasamy, K.; Malik, M. A.; O'Brien, P. *Chem. Sci.* **2011**, *2* (6), 1170−1172.

(3) (a) Brennan, J. G.; Siegrist, T.; Stuczynski, S. M.; Steigerwald, M. L. *J. Am. Chem. Soc.* **1989**, *111* (26), 9240−9241. (b) Murray, C. B.; Kagan, C. R.; Bawendi, M. G. *Annu. Rev. Mater. Sci.* **2000**, *30*, 545−610. (c) Murray, C. B.; Norris, D. J.; Bawendi, M. G. *J. Am. Chem. Soc.* **1993**, *115* (19), 8706−8715.

(4) (a) Ki, W.; Li, J. *J. Am. Chem. Soc.* **2008**, *130* (26), 8114−8120. (b) Huang, X. Y.; Roushan, M.; Emge, T. J.; Bi, W. H.; Thiagarajan, S.; Cheng, J. H.; Yang, R. G.; Li, J. *Angew. Chem., Int. Ed.* **2009**, *48* (42), 7871−7874.

(5) (a) Berger, R.; Resnati, G.; Metrangolo, P.; Weber, E.; Hulliger, J. *Chem. Soc. Rev.* **2011**, *40* (7), 3496−3508. (b) Chan, M. C. W. *Macromol. Chem. Phys.* **2007**, *208* (17), 1845−1852. (c) Dias, H. V. R.; Fianchini, M. *Comments Inorg. Chem.* **2007**, *28* (1−2), 73−92. (d) Plenio, H. *ChemBioChem* **2004**, *5* (5), 650−655. (e) Witt, M.; Roesky, H. W. *Prog. Inorg. Chem.* **1992**, *40*, 353−444.

(6) (a) Britovsek, G. J. P.; Ugolotti, J.; White, A. J. P. *Organometallics* **2005**, *24* (7), 1685−1691. (b) Whitmire, K. H.; Hoppe, S.; Sydora, O.; Jolas, J. L.; Jones, C. M. *Inorg. Chem.* **2000**, *39* (1), 85−97. (c) Jones, C. M.; Burkart, M. D.; Bachman, R. E.; Serra, D. L.; Hwu, S. J.; Whitmire, K. H. *Inorg. Chem.* **1993**, *32* (23), 5136−5144. (d) Abbott, R. G.; Cotton, F. A.; Falvello, L. R. *Inorg. Chem.* **1990**, *29* (3), 514−521. (e) Campbell, C.; Bott, S. G.; Larsen, R.; Vandersluys, W. G. *Inorg. Chem.* **1994**, 33 (22), 4950−4958. (f) Kim, M.; Zakharov, L. N.; Rheingold, A. L.; Doerrer, L. H. *Polyhedron* **2005**, *24* (14), 1803−1812. (g) Metz, M. V.; Sun, Y. M.; Stern, C. L.; Marks, T. J. *Organometallics* **2002**, *21* (18), 3691−3702. (h) Buzzeo, M. C.; Iqbal, A. H.; Long, C. M.; Millar, D.; Patel, S.; Pellow, M. A.; Saddoughi, S. A.; Smenton, A. L.; Turner, J. F. C.; Wadhawan, J. D.; Compton, R. G.; Golen, J. A.; Rheingold, A. L.; Doerrer, L. H. *Inorg. Chem.* **2004**, *43* (24), 7709−7725. (i) Norton, K.; Kumar, G. A.; Dilks, J. L.; Emge, T. J.; Riman, R. E.; Brik, M. G.; Brennan, J. G. *Inorg. Chem.* **2009**, *48* (8), 3573−3580. (j) Norton, K.; Emge, T. J.; Brennan, J. G. *Inorg. Chem.* **2007**, *46* (10), 4060−4066. (k) Schnaars, D. D.; Wu, G.; Hayton, T. W. *Dalton Trans.* **2009**, *19*, 3681−3687. (l) Fortier, S.; Wu, G.; Hayton, T. W. *Inorg. Chem.* **2009**, *48* (7), 3000−3011.

(7) (a) Peach, M. E. *J. Inorg. Nucl. Chem.* **1973**, *35* (3), 1046−1048. (b) Peach, M. E. *Can. J. Chem.* **1968**, *46* (16), 2699−2706. (c) Chadwick, S.; Englich, U.; Noll, B.; Ruhlandt-Senge, K. *Inorg. Chem.* **1998**, *37* (18), 4718−4725. (d) De Mel, V. S. J.; Kumar, R.; Oliver, J. P. *Organometallics* **1990**, *9* (4), 1303−1307. (e) Hendershot, D. G.; Kumar, R.; Barber, M.; Oliver, J. P. *Organometallics* **1991**, *10* (6), 1917−1922. (f) Carlton, L.; Tetana, Z. N.; Fernandes, M. A. *Polyhedron* **2008**, *27* (8), 1959−1962. (g) Melman, J. H.; Emge, T. J.; Brennan, J. G. *Inorg. Chem.* **2001**, *40* (5), 1078−1085. (h) Melman, J. H.; Rohde, C.; Emge, T. J.; Brennan, J. G. *Inorg. Chem.* **2002**, *41* (1), 28−33. (i) Kumar, G. A.; Riman, R. E.; Diaz-Torres, L. A. D.; Barbosa-Garcia, O. B.; Banerjee, S.; Kornienko, A.; Brennan, J. G. *Chem. Mater.* **2005**, *17* (20), 5130−5135. (j) Banerjee, S.; Kumar, G. A.; Emge, T. J.; Riman, R. E.; Brennan, J. G. *Chem. Mater.* **2008**, *20* (13), 4367−4373. (k) Banerjee, S.; Huebner, L.; Romanelli, M. D.; Kumar, G. A.; Riman, R. E.; Emge, T. J.; Brennan, J. G. *J. Am. Chem. Soc.* **2005**, *127* (45), 15900−15906.

(8) Klapotke, T. M.; Krumm, B.; Polborn, K. *Eur. J. Inorg. Chem.* **1999**, *8*, 1359−1366.

(9) (a) Davidson, J. L.; Holz, B.; Leverd, P. C.; Lindsell, E. W.; Simpson, N. J. *J. Chem. Soc., Dalton Trans.* **1994**, *24*, 3527−3532.

DOI: 10.1021/acs.inorgchem.5b00452
Inorg. Chem. 2015, 54, 8896−8904

(b) Krogh-Jespersen, K.; Romanelli, M. D.; Melman, J. H.; Emge, T. J.; Brennan, J. G. *Inorg. Chem.* **2010**, *49* (2), 552−560.
(10) Emge, T. J.; Romanelli, M. D.; Moore, B. F.; Brennan, J. G. *Inorg. Chem.* **2010**, *49* (16), 7304−7312.
(11) Estudiante-Negrete, F.; Redon, R.; Hernandez-Ortega, S.; Toscano, R. A.; Morales-Morales, D. *Inorg. Chim. Acta* **2007**, *360* (5), 1651−1660.
(12) (a) Uson, M. A.; Llanos, J. M. *J. Organomet. Chem.* **2002**, *663* (1−2), 98−105. (b) Basauri-Molina, M.; Hernandez-Ortega, S.; Toscano, R. A.; Valdes-Martinez, J.; Morales-Morales, D. *Inorg. Chim. Acta* **2010**, *363* (6), 1222−1229. (c) Corona-Rodriguez, M.; Hernandez-Ortega, S.; Valdes-Martinez, J.; Morales-Morales, D. *Supramol. Chem.* **2007**, *19* (8), 579−563. (d) Herrera-Alvarez, C.; Hernandez-Ortega, S.; Morales-Morales, D. *Acta Crystallogr., Sect. E: Struct. Rep. Online* **2007**, *e63* (5), m1490. (e) Garces-Rodriguez, A.; Morales-Morales, D.; Hernandez-Ortega, S. *Acta Crystallogr., Sect. E: Struct. Rep. Online* **2007**, *e63* (2), m479.
(13) (a) Kacprzak, J. *Pr. Inst. Hutn.* **1959**, *11*, 167−92. (b) Tonejc, A.; Ogorelec, Z.; Mestnik, B. *J. Appl. Crystallogr.* **1975**, *8*, 375−379. (c) Liu, C. W.; Stubbs, T.; Staples, R. J.; Fackler, J. P. *J. Am. Chem. Soc.* **1995**, *117* (38), 9778−9779.
(14) Popovic, S.; Tonejc, A.; Grzeta-Plenkovic, B.; Celustka, B.; Trojko, R. *J. Appl. Crystallogr.* **1979**, *12* (4), 416−420.
(15) Palatnik, L. S.; Levitin, V. V. *Dokl. Akad. Nauk SSSR* **1954**, *96*, 975−978.
(16) Savitsky, E. M.; Terekhova, V. F. *Dokl. Akad. Nauk* **1949**, *68*, 344−349.
(17) *SADABS, BrukerNonius area detector scaling and absorption correction,* version 2.05; Bruker AXS Inc: Madison, WI, 2003.
(18) Sheldrick, G. M. *SHELXS86, Program for the Solution of Crystal Structures;* University of Göttingen: Germany, 1986.
(19) (a) Sheldrick, G. M. *Acta Crystallogr., Sect. A: Found. Crystallogr.* **2008**, *64*, 112−120. (b) Sheldrick, G. M. *SHELXL97, Program for Crystal Structure Refinement;* University of Göttingen: Germany, 1997.
(20) CCDC Program Mercury. Macrae, C. F.; Bruno, I. J.; Chisholm, J. A.; Edgington, P. R.; McCabe, P.; Pidcock, E.; Rodriguez-Monge, L.; Taylor, R.; van de Streek, J.; Wood, P. A. *J. Appl. Crystallogr.* **2008**, *41*, 466−469.10.1107/S0021889807067908
(21) *Program POV-Ray. Persistence of Vision Raytracer (Version 3.6);* Persistence of Vision Pty. Ltd: Williamstown, Victoria, Australia, 2004, retrieved from http://www.povray.org/download/.
(22) Dennington, R.; Keith, T.; Millam, J., *GaussView, Version 5;* Semichem Inc: Shawnee Mission, KS, 2009.
(23) Frisch, M. J.; Trucks, G. W.; Schlegel, H. B.; Scuseria, G. E.; Robb, M. A.; Cheeseman, J. R.; Scalmani, G.; Barone, V.; Mennucci, B.; Petersson, G. A.; Nakatsuji, H.; Caricato, M.; Li, X.; Hratchian, H. P.; Izmaylov, A. F.; Bloino, J.; Zheng, G.; Sonnenberg, J. L.; Hada, M.; Ehara, M.; Toyota, K.; Fukuda, R.; Hasegawa, J.; Ishida, M.; Nakajima, T.; Honda, Y.; Kitao, O.; Nakai, H.; Vreven, T.; Montgomery, J. A., Jr.; Peralta, J. E.; Ogliaro, F.; Bearpark, M.; Heyd, J. J.; Brothers, E.; Kudin, K. N.; Staroverov, V. N.; Kobayashi, R.; Normand, J.; Raghavachari, K.; Rendell, A.; Burant, J. C.; Iyengar, S. S.; Tomasi, J.; Cossi, M.; Rega, N.; Millam, J. M.; Klene, M.; Knox, J. E.; Cross, J. B.; Bakken, V.; Adamo, C.; Jaramillo, J.; Gomperts, R.; Stratmann, R. E.; Yazyev, O.; Austin, A. J.; Cammi, R.; Pomelli, C.; Ochterski, J. W.; Martin, R. L.; Morokuma, K.; Zakrzewski, V. G.; Voth, G. A.; Salvador, P.; Dannenberg, J. J.; Dapprich, S.; Daniels, A. D.; Farkas, Ö.; Foresman, J. B.; Ortiz, J. V.; Cioslowski, J.; Fox, D. J., *Gaussian09,* Revision D.01; Gaussian, Inc: Wallingford, CT, 2009.
(24) Parr, R. G.; Yang, W. *Density-Functional Theory of Atoms and Molecules;* University Press: Oxford, 1989.
(25) (a) Zhao, Y.; Truhlar, D. G. *Theor. Chem. Acc.* **2008**, *120* (1−3), 215−241. (b) Zhao, Y.; Truhlar, D. G. *Chem. Phys. Lett.* **2011**, *502*, 1−7. (c) Zhao, Y.; Truhlar, D. G. *Acc. Chem. Res.* **2008**, *41*, 157−163.
(26) Perdew, J. P.; Burke, K.; Ernzerhof, M. *Phys. Rev. Lett.* **1996**, *77* (18), 3865−3868.
(27) (a) Lee, C. T.; Yang, W. T.; Parr, R. G. *Phys. Rev. B: Condens. Matter Mater. Phys.* **1988**, *37* (2), 785−789. (b) Becke, A. D. *J. Chem. Phys.* **1993**, *98*, 5648−5650.
(28) Wadt, W. R.; Hay, P. J. *J. Chem. Phys.* **1985**, *82* (1), 284−298.
(29) Roy, L. E.; Hay, P. J.; Martin, R. L. *J. Chem. Theory Comput.* **2008**, *4* (7), 1029−1031.
(30) Martin, J. M. L.; Sundermann, A. *J. Chem. Phys.* **2001**, *114* (8), 3408−3420.
(31) (a) Ditchfield, R.; Hehre, W. J.; Pople, J. A. *J. Chem. Phys.* **1971**, *54* (2), 724−728. (b) Hariharan, P. C.; Pople, J. A. *Mol. Phys.* **1974**, *27* (1), 209−214. (c) Krishnan, R.; Binkley, J. S.; Seeger, R.; Pople, J. A. *J. Chem. Phys.* **1980**, *72* (1), 650−654. (d) Clark, T.; Chandrasekhar, J.; Spitznagel, G. W.; Schleyer, P. R. *J. Comput. Chem.* **1983**, *4* (3), 294−301.
(32) Weinhold, F. L.; Landis, C. *Valency and Bonding: A Natural Bond Orbital Donor-Acceptor Perspective;* Cambridge University Press: Cambridge, U.K., 2005.
(33) Glendening, E. D.; Badenhoop, J. K.; Reed, A. E.; Carpenter, J. E.; Bohmann, J. A.; Morales, C. M.; Weinhold, F. *NBO 5.0;* Theoretical Chemistry Institute: University of Wisconsin: Madison, WI, 2001.
(34) (a) Chadha, R. K.; Kumar, R.; Tuck, D. G. *Can. J. Chem.* **1987**, *65* (6), 1336−1342. (b) Chen, C. H.; Weng, Z. Q.; Hartwig, J. F. *Organometallics* **2012**, *31* (22), 8031−8036. (c) Dance, I. G.; Guerney, P. J.; Rae, A. D.; Scudder, M. L. *Inorg. Chem.* **1983**, *22* (20), 2883−2887. (d) Ohlmann, D.; Marchand, C. M.; Schoenberg, H.; Gruetzmacher, H.; Pritzkow, H. *Z. Anorg. Allg. Chem.* **1996**, *622* (8), 1349−1357. (e) Yam, V. W. W.; Lam, C. H.; Fung, W. K. M.; Cheung, K. K. *Inorg. Chem.* **2001**, *40* (14), 3435−3442. (f) Bonasia, P. J.; Mitchell, G. P.; Hollander, F. J.; Arnold, J. *Inorg. Chem.* **1994**, *33* (9), 1797−1802. (g) Cheng, Y.; Emge, T. J.; Brennan, J. G. *Inorg. Chem.* **1996**, *35* (25), 7339−7344. (h) Rodriguez, A.; Romero, J.; Garcia-Vasquez, J. A.; Duran, M. L.; Sousa-Pedrares, A.; Sousa, A.; Zubieta, J. *Inorg. Chim. Acta* **1999**, *284* (1), 133−138. (i) Low, K. H.; Li, C. H.; Roy, V. A. L.; Chui, S. S. Y.; Chan, S. L. F.; Che, C. M. *Chem. Science* **2010**, *1* (4), 515−518. (j) Sharma, R. K.; Kedarnath, G.; Jain, V. K.; Wadawale, A.; Pillai, C. G. S.; Nalliath, M.; Vishwanadh, B. *Dalton Trans.* **2011**, *40* (36), 9194−9201. (k) Allen, F. H. *Acta Crystallogr., Sect. B: Struct. Sci.* **2002**, *58*, 380−388.
(35) (a) Kitajima, N.; Fujisawa, K.; Tanaka, M.; Morooka, Y. *J. Am. Chem. Soc.* **1992**, *114* (23), 9232−9233. (b) Beck, W.; Stetter, K. H. *Inorg. Nucl. Chem. Lett.* **1966**, *2* (12), 383−387.
(36) Addison, A. W.; Sinn, E. *Inorg. Chem.* **1983**, *22* (8), 1225−1228.
(37) Plevin, M. J.; Bryce, D. L.; Boisbouvier, J. *Nat. Chem.* **2010**, *2* (6), 466−471.
(38) (a) Vyas, N. K.; Vyas, M. N.; Quiocho, F. A. *Science* **1988**, *242* (4883), 1290−1295. (b) Tsuzuki, S.; Fujii, A. *Phys. Chem. Chem. Phys.* **2008**, *10* (19), 2584−94.
(39) Kaminaris, D. M.; Galinos, A. G. *Acta Chim. Acad. Sci. Hung.* **1978**, *98* (3), 293−298.
(40) Heeg, M. G.; Yearwood, B.; Oliver, J. *Private Communication,* 2010.
(41) Ruhlandtsenge, K.; Bartlett, R. A.; Olmstead, M. M.; Power, P. P. *Inorg. Chem.* **1993**, *32* (9), 1724−1728.
(42) Kuchta, M. C.; Rheingold, A. L.; Parkin, G. *New J. Chem.* **1999**, *23* (10), 957−959.
(43) Smith, D. M.; Ibers, J. A. *Polyhedron* **1998**, *17* (11−12), 2105−2108.
(44) Cheng, Y. F.; Emge, T. J.; Brennan, J. G. *Inorg. Chem.* **1994**, *33* (17), 3711−3714.
(45) (a) Schlecht, S.; Budde, M.; Kienle, L. *Inorg. Chem.* **2002**, *41* (23), 6001−6005. (b) Rekken, B. D.; Brown, T. M.; Fettinger, J. C.; Lips, F.; Tuononen, H. M.; Herber, R. H.; Power, P. P. *J. Am. Chem. Soc.* **2013**, *135* (27), 10134−10148. (c) Eichhofer, A.; Jiang, J. J.; Sommer, H.; Weigend, F.; Fuhr, O.; Fenske, D.; Su, C. Y.; Buth, G. *Eur. J. Inorg. Chem.* **2010**, *3*, 410−418. (d) Seligson, A. L.; Arnold, J. *J. Am. Chem. Soc.* **1993**, *115* (18), 8214−8220. (e) Kedarnath, G.; Kumbhare, L. B.; Dey, S.; Wadawale, A. P.; Jain, V. K.; Dey, G. K. *Polyhedron* **2009**, *28* (13), 2749−2753.
(46) Appleton, S. E.; Briand, G. G.; Decken, A.; Smith, A. S. *Acta Crystallogr., Sect. E: Struct. Rep. Online* **2011**, *e67*, m714−m721.

DOI: 10.1021/acs.inorgchem.5b00452
Inorg. Chem. 2015, 54, 8896−8904

(47) (a) Eychenne-Baron, C.; Ribot, F.; Steunou, N.; Sanchez, C.; Fayon, F.; Biesemans, M.; Martins, J. C.; Willem, R. *Organometallics* **2000**, *19* (10), 1940−1949. (b) Zabula, A. V.; Filatov, A. S.; Petrukhina, M. A. *J. Cluster Sci.* **2010**, *21* (3), 361−370. (c) Plasseraud, L.; Cattey, H.; Richard, P. *Z. Naturforsch., B: J. Chem. Sci.* **2011**, *66* (3), 262−268. (d) Barbul, I.; Johnson, A. L.; Kociok-Kohn, G.; Molloy, K. C.; Silvestru, C.; Sudlow, A. L. *ChemPlusChem* **2013**, *78* (8), 866−874.
(48) Rekken, B. D.; Brown, T. M.; Olmstead, M. M.; Fettinger, J. C.; Power, P. P. *Inorg. Chem.* **2013**, *52* (6), 3054−3062.
(49) Cheng, Y. F.; Emge, T. J.; Brennan, J. G. *Inorg. Chem.* **1996**, *35* (2), 342−346.
(50) Wiberg, K. B. *Tetrahedron* **1968**, *24*, 1083−1096.
(51) Sculfort, S.; Braunstein, P. *Chem. Soc. Rev.* **2011**, *40*, 2741−2760.

DOI: 10.1021/acs.inorgchem.5b00452
Inorg. Chem. 2015, 54, 8896−8904